Highly rotational C_{60} dynamics inside single-walled carbon nanotubes: NMR observations

K. Matsuda,[1] Y. Maniwa,[1,3] and H. Kataura[2,3]
[1]*Faculty of Science, Tokyo Metropolitan University, 1-1 Minami-osawa, Hachioji, Tokyo 192-0397, Japan*
[2]*Nanotechnology Research Institute, National Institute of Advanced Industrial Science and Technology (AIST), Central 4, Higashi1-1-1, Tsukuba 305-8562, Japan*
[3]*JST, CREST, 4-1-8 Hon-Chou, Kawaguchi, Saitama 332-0012, Japan*
(Received 18 October 2007; published 21 February 2008)

Rotational dynamics of C_{60} molecules composing a one-dimensional (1D) linear array inside single-walled carbon nanotubes have been investigated by ^{13}C NMR in a temperature range from 4.2 to 300 K. The temperature dependence of the NMR lineshape and spin-lattice relaxation time (T_1) indicate that the encapsulated C_{60} molecules exhibit a quasi-free-rotation with correlation times of 5–10 ps at 300 K. With decreasing temperature, the large amplitude molecular rotation continues to 30 K with an activation energy of 467 K. It is suggested that the C_{60} linear array does not undergo an orientational phase transition, which is associated with its 1D nature. Furthermore, no evidence for the polymerization of C_{60} molecules is found from the ^{13}C NMR line shape analysis.

DOI: 10.1103/PhysRevB.77.075421 PACS number(s): 61.48.−c, 81.07.De, 76.60.−k, 64.70.Nd

I. INTRODUCTION

Single-walled carbon nanotubes (SWCNTs) encapsulate many kinds of materials in their inner hollow cavities with a typical diameter of 1 nm.[1] Materials confined in such small cavities are expected to show novel features that are not observed in bulk materials.[2–6] Among this class of materials, SWCNTs filled with fullerenes (e.g., C_{60}), so-called "peapods"[7] in which fullerene molecules form a quasi-one-dimensional (1D) array, have attracted considerable attention due to their peculiar electronic properties.[8–10] In alkali-doped C_{60} peapods, for example, occurrence of superconductivity has been predicted.[10] However, the structural properties of C_{60} peapods have not yet been fully understood.

In particular, because the C_{60} linear arrays inside SWCNTs with typical diameters ($2R$) of around 13.5 Å may be treated as an ideal 1D crystal, a C_{60}-ordered structure should not be achieved at finite temperature (T). Indeed, theoretical calculations predict the C_{60} molecules inside a SWCNT behave like a 1D molecular liquid down to low T, although having the specific energetically favorable orientation of C_{60}.[11,12] In the case of a C_{70} 1D array formed inside a SWCNT, x-ray diffraction (XRD) experiments and their analysis within an Ising model for molecular orientation indicate that the long-range orientational ordering of C_{70} molecules cannot be realized at finite T.[13,14] The orientational properties of the C_{60} three-dimensional (3D) crystal, on the other hand, were investigated in detail: solid C_{60} undergoes a first-order phase transition from the orientationally disordered fcc phase at high T to the orientationally ordered sc phase at critical T, $T_C \sim 260$ K.[15] This orientational phase transition is accompanied by a drastic change in the C_{60} rotational dynamics. Below T_C, the rapid quasi-free-rotation of C_{60} is repressed and the C_{60} ratchets between preferred orientations.

Polymerization of the C_{60} molecules inside SWCNTs has also been suggested by several experiments. Raman spectroscopic results indicated photopolymerization of the encapsulated C_{60} molecules under a 488 nm laser irradiation.[16] C_{60} polymerization inside SWCNTs was also observed by high-resolution transmission electron microscope (TEM).[17] Another polymerization route, where high-T treatment under high pressure is employed, was found by XRD experiments.[18–20] While these experiments employ either high energy irradiation or high pressure, an inelastic neutron scattering experiment interestingly suggested that as-synthesized C_{60} peapods are filled with a mix of C_{60} monomers and polymers at ambient pressure without any high energy irradiation.[21]

In this context, we carried out a systematic study of an "as-prepared" C_{60} peapod sample by ^{13}C NMR in a wide T range between 4.2 and 300 K, and report the structural and molecular orientational dynamics of C_{60} inside SWCNTs. It is clarified that the C_{60} molecules inside SWCNTs exhibit large amplitude molecular rotations down to 30 K, which is much less than 130–150 K in C_{60}, C_{70}, and C_{76} fullerene solids.

II. EXPERIMENT

C_{60} peapods were prepared by a vapor reaction method[16] using highly purified SWCNTs (mean diameter $2R=13.8$ Å, $\sigma=1$ Å). The starting raw materials were fabricated by a pulsed laser ablation method with a Ni/Co-catalyzed carbon rod containing naturally abundant (~1.1 %) ^{13}C isotope. The pristine C_{60} materials were nominally ~30% ^{13}C enriched in order to increase the ^{13}C NMR signal from the encapsulated C_{60}. To remove condensed C_{60} molecules outside the SWCNT bundles, the reacted SWCNTs with C_{60} vapor were heated at 550 °C under dynamic vacuum for 1 h. For the NMR measurements, the C_{60} peapod samples (~25 mg) were set inside a quartz NMR tube. Samples prepared using essentially the same technique have been characterized by XRD, Raman, and TEM observations.[13,14,16] The XRD measurements confirmed the formation of C_{60} 1D arrays with a mean C_{60}-intermolecular distance (center to center) of 9.5 Å inside SWCNTs. The NMR experiments were performed in external fields of 4.0 and 9.3 T using a

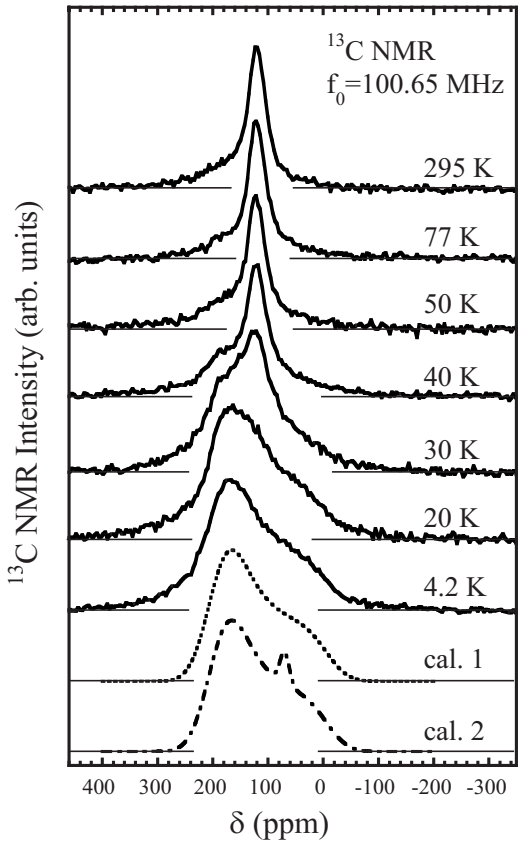

FIG. 1. Temperature evolution of ^{13}C NMR spectrum for C_{60} molecules encapsulated inside SWCNTs. A calculated powder pattern line shape with CS tensor $(\delta_{11}, \delta_{22}, \delta_{33})=(208, 177, -8)$ ppm is also displayed in the figure (cal. 1). The line shape is convoluted with a Gaussian function with a FWHM value of 70 ppm. The line shape expected for the [2+2] cycloadditive C_{60} dimers inside SWCNTs is displayed at the bottom of the figure (cal. 2). In this simulation, the signal intensity ratio of sp^2 and sp^3 carbons is 2:58 and the line shape from sp^3 carbon was assumed to be a Gaussian function with a peak at 70 ppm and FWHM value of 20 ppm.

conventional phase-coherent pulsed spectrometer. ^{13}C NMR spectra were taken by Fourier transforming the latter half of the spin-echo signal following the $\pi/2$-π pulse sequence. The typical $\pi/2$ pulse widths were 9.5 and 7.0 μs at 4.0 and 9.3 T, respectively. The value of the nuclear spin-lattice relaxation time (T_1) was measured by monitoring the recovery of ^{13}C nuclear magnetization with time $M(t)$ after the saturation pulses.

III. RESULTS AND DISCUSSION

Figure 1 presents the T evolution of the ^{13}C NMR spectrum for C_{60} peapods measured at 9.3 T. The ratio of the ^{13}C isotope amounts included in SWCNTs and encapsulated C_{60} was roughly estimated to be 1:9, assuming the bulk filling factor to be ~85% of the C_{60} molecules.[13] Therefore, the observed NMR spectrum is assigned almost completely to the encapsulated C_{60}.

A. ^{13}C NMR spectra at low temperatures

At low T below 25 K, the ^{13}C NMR spectrum shows a typical chemical-shift-anisotropy (CSA) powder line shape for sp^2 carbon, as shown in Fig. 1.[22] The line shape at 4.2 K can be well reproduced by a calculation using a chemical shift (CS) tensor with principal values $\delta_{11}=203$ ppm, $\delta_{22}=177$ ppm, and $\delta_{33}=-8$ ppm. Essentially the same powder line shape has been obtained for the low T phase of C_{60} bulk crystal.[23–25]

Furthermore, the spectra indicate that almost all the carbon atoms are sp^2 carbon. When the C_{60} molecules inside SWCNTs are polymerized or dimerized through [2+2] cycloaddition as in bulk C_{60} polymers,[26,27] 6.7% and 3.3% of the total carbons must be transformed to sp^3 carbons for ideal infinite polymerization and dimerization, respectively. Here, it should be noted that the sp^3 carbons have a characteristically small CSA (<30 ppm) due to the high symmetry of their electronic environment and are consequently seen as a relatively sharp feature in the spectra. Therefore, if C_{60} molecules are polymerized inside SWCNTs, a narrow NMR spectrum arising from sp^3 carbons appears on the broad powder NMR pattern for sp^2 carbon. Such NMR spectra were actually observed in bulk C_{60} polymers.[28] Here, we tentatively simulated a powder line shape for C_{60} dimers where the signal intensity ratio of sp^2 and sp^3 carbons is 58:2. The result is shown at the bottom of Fig. 1. The line shape from sp^3 carbon was assumed to be a Gaussian with a peak at 70 ppm and full width at half maximum (FWHM) of 20 ppm. It is concluded from a comparison of the simulated pattern with the observed spectra that the volume fraction of dimers (or polymers), if present, must be much smaller than ~20% (or 10%).

B. ^{13}C NMR spectra at high temperatures: Motional narrowing

Above ~30 K, the observed spectra are substantially narrower than that for typical sp^2 carbons and those observed at lower T, as shown in Fig. 1. This indicates that large amplitude C_{60} rotations, whose rotation angles are larger than $\sim\pi$ within the NMR time scale given by the inverse of static linewidth, $(2\pi\times 20\ \text{kHz})^{-1}\sim 8\times 10^{-6}$ s, occur above 30 K. Such large rotational motion averages out the CSA and results in the motional narrowing of the powder spectrum.[22]

Figure 2(a) shows an example of the motionally narrowed spectrum observed at 77 K. The spectrum exhibits a slight tail on the low-field side. As shown in Fig. 1, qualitatively the same line shape is observed at 295 K. The line shape can be reconstructed by a superposition of two components: a narrow component corresponding to rotating C_{60} molecules and a broad component. The broad component, of which spectral intensity is ~15% of the total intensity, is probably assigned to carbon in SWCNTs. Therefore, attention is focused on the motionally narrowed component. In Fig. 2, the broad component [dotted gray line in Fig. 2(a)] was subtracted from the measured spectrum to gain the narrow component [solid gray line in Fig. 2(a)]. In the subtraction, the calculated CSA line shape for typical sp^2 carbon (dotted line in Fig. 1) was used as the broad component. The derived narrow component is well fitted by a Lorentzian with a FWHM of 35 ppm, as shown in Fig. 2(b), indicating molecular rotation faster than the NMR linewidth. The finite line-

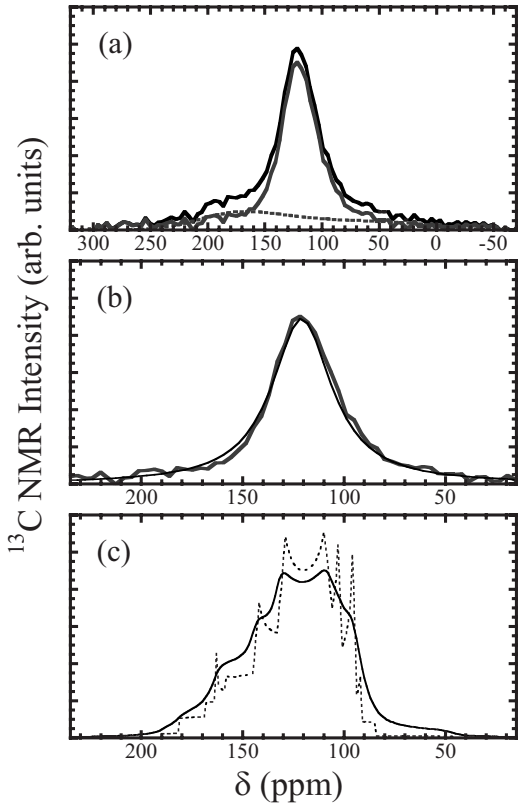

FIG. 2. (a) ^{13}C NMR spectrum observed at 77 K. The motionally narrowed component (solid gray line) was deduced by subtracting the broad component (dotted gray line) from the measured spectrum (solid line). (b) A Lorentzian fit to the narrow spectral component at 77 K. The narrow component (solid gray line) is well fitted by a Lorentzian function with a FWHM value of 35 ppm (thin solid line). (c) Simulated line shape for the uniaxial rotation. The motionally averaged line shape was calculated for the rotation along the twofold axis of the C_{60} molecule (thin dotted line) (see text for details). The line shape convoluted by a Lorentzian function with a FWHM value of 7 ppm is also displayed (thin solid line).

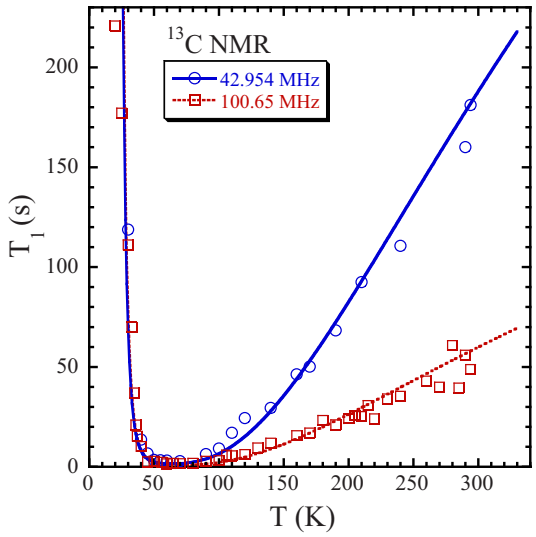

FIG. 3. (Color online) Temperature and frequency dependence of ^{13}C nuclear spin-lattice relaxation time T_1 of encapsulated C_{60} measured at 4.0 T (circles) and 9.4 T (squares). The solid and dotted lines represent the best fits to the T_1 data at 4.0 and 9.4 T, respectively.

width possibly originates from inhomogeneous line broadening due to the magnetic catalysts contained as impurities and the anisotropic susceptibility of SWCNTs.

The effect of C_{60} polymerization or anisotropic C_{60} rotational motion on the motionally narrowed NMR lineshape is now discussed. In the 1D polymer (or dimer) inside SWCNTs, the rotational freedom of the polymerized (or dimerized) molecules should be restricted due to the geometry; the C_{60} polymers cannot undergo isotropic rotation but can undergo uniaxial rotation around the tube axis. The interaction between C_{60} and the SWCNT wall may also cause an anisotropic C_{60} rotational motion inside SWCNTs. Here, the uniaxial rotation case is discussed as the most probable anisotropic rotation, in which the CS tensor is time averaged around the rotational axis in the NMR time scale.

The uniaxial rotation along the twofold axis of the C_{60} molecule is considered as an example. This rotational axis is coincident with the molecular long axis of [2+2] cycloadditive 1D C_{60} polymer. Furthermore, the CS tensor of sp^2 carbon in the C_{60} molecule is approximated to an axially symmetric CS tensor of $\delta_{11}=\delta_{22}=(203+177)/2=180$ ppm and $\delta_{33}=-8$ ppm. The anisotropy of the time-averaged CS tensor $(\delta'_{11},\delta'_{22},\delta'_{33})$ is then written as $(\delta'_{33}-\delta'_{22})=(3\cos^2\theta-1)(\delta_{33}-\delta_{22})/2$, where θ is the angle between the rotational and the δ_{33} axes.[29] The resultant δ'_{33} axis is parallel to the rotational axis. The isotropic CS must be invariant with the molecular rotation, namely, $(\delta_{11}+\delta_{22}+\delta_{33})/3=(\delta'_{11}+\delta'_{22}+\delta'_{33})/3$. In Fig. 2(c), the calculated line shape for the sp^2 carbon in C_{60} dimers is shown. The line shape is a superposition of signals from eight nonequivalent carbon sites relative to the molecular rotational axis. It is found that the resulting line shape is asymmetric with a FWHM of ~60 ppm and quite different from the observed symmetrical pattern with a FWHM of 35 ppm. For other rotational axes such as the threefold axis of the C_{60} molecule, essentially the same spectra can be obtained. Hence, the calculation fails to reproduce the observed line shape, indicating that the C_{60} molecules do not undergo uniaxial rotation inside SWCNTs. As shown in Fig. 2(b), the observed line shape is a symmetric one expected for an isotropic (3D) rotation. These results show that almost all the encapsulated C_{60} molecules exist as monomers, which is consistent with the absence of the sp^3 signal in the NMR spectra.

The results reveal that polymerization of the encapsulated C_{60} molecules does not occur under the present NMR condition without any high energy irradiation, which is different from TEM and Raman experiments.[16,17] The present results should be consistent with a recent energy calculation that indicates an energy barrier of ~1.3 eV for converting C_{60} monomers to C_{60} dimers even inside SWCNTs.[30]

C. ^{13}C NMR spin-lattice relaxation time T_1

To gain more insight into C_{60} dynamics, T_1 was measured using ^{13}C NMR at 4.0 and 9.3 T. In Fig. 3, the values of T_1 are plotted as a function of T. T_1 has a minimum at ~60 K.

At high T, the T_1 values are dependent on the Larmor frequency, $\omega/2\pi$. This T_1 behavior indicates that the nuclear relaxation is caused by a fluctuating local field at the ^{13}C site due to the rotational motion of C_{60} molecules. In the present case, there are two dominant origins for the local fields responsible for the T_1 mechanism: CSA and nuclear dipole-dipole interactions.

The CSA contribution to T_1^{-1}, $T_{1\mathrm{CSA}}^{-1}$ is first considered. In the case of isotropic molecular rotation, $T_{1\mathrm{CSA}}^{-1}$ can be expressed in terms of the effective rotational correlation time τ as

$$T_{1\mathrm{CSA}}^{-1} = \frac{3}{20}\gamma^2 B_0{}^2 \Delta^2 \left(1 + \frac{\eta^2}{3}\right) \frac{2\tau}{1+\omega^2\tau^2}, \tag{1}$$

where γ is the ^{13}C gyromagnetic ratio, $\omega = \gamma B_0$ is the angular Larmor frequency, $\Delta = (2\delta_{33} - \delta_{11} - \delta_{22})/3$, and $\eta = (\delta_{11} - \delta_{22})/\Delta$.[22–25] Here, $\Delta = 132$ ppm and $\eta = 0.2$ are used. In addition to Eq. (1), antisymmetric components of the CS tensor also contribute to T_1^{-1}. However, this contribution seems to be relatively small, although it has not been determined experimentally. Thus, it is assumed that the antisymmetric contribution to T_1^{-1} can be ignored. It should be noted that $T_{1\mathrm{CSA}}^{-1}$ increases proportional to B_0^2 for the limit of short correlation time $\omega\tau \ll 1$ and becomes field independent for $\omega\tau \gg 1$. As seen in Fig. 3, the observed T_1 is field dependent at high T and the average ratio of T_1 obtained at 9.4 and 4.0 T above $\sim$170 K, $T_1^{4.0\ \mathrm{T}}/T_1^{9.4\ \mathrm{T}} \sim 3.2$, is close to the square of the ratio of the measured fields, $(9.4/4.0)^2 \sim 5.5$. This result suggests that the CSA mechanism dominantly contributes to the ^{13}C nuclear relaxation. Indeed, the CSA relaxation can account for most of the obtained T_1^{-1} values; the CSA contribution is estimated to be $\sim$85% of the total T_1^{-1} at 9.4 T.

Since ^{13}C isotopically enriched C_{60} molecules were employed in the present experiments, the ^{13}C homonuclear dipolar interaction considerably contributed to the ^{13}C nuclear relaxation in addition to the above CSA mechanism. The relaxation rate, $T_{1\mathrm{dip}}^{-1}$, caused by the fluctuation in the dipolar interaction is represented as[22]

$$T_{1\mathrm{dip}}^{-1} = \frac{2}{3} M_{2\mathrm{dip}} \left(\frac{\tau}{1+\omega^2\tau^2} + \frac{4\tau}{1+4\omega^2\tau^2} \right). \tag{2}$$

Here, $M_{2\mathrm{dip}}$ is the ^{13}C NMR second moment owing to ^{13}C dipolar interactions. For the evaluation of $T_{1\mathrm{dip}}^{-1}$ in ^{13}C isotopically enriched samples, the mean value of $M_{2\mathrm{dip}}$, $\langle M_{2\mathrm{dip}} \rangle$, was calculated using the method of moments by Van Vleck.[31] Here, the contribution from the nearest-neighbor carbons is taken into consideration. In a C_{60} molecule, each carbon has three nearest-neighbor carbons. Therefore, $\langle M_{2\mathrm{dip}} \rangle$ is given by

$$\langle M_{2\mathrm{dip}} \rangle = \sum_{n=1,2,3} \frac{3}{20\pi^2} n P(n) \gamma^4 h^2 I(I+1) \left(\frac{1}{r_{\mathrm{C\text{-}C}}} \right)^6, \tag{3}$$

where I is the spin quantum number (in this case, $I = 1/2$), h the Planck constant, $r_{\mathrm{C\text{-}C}}$ the nearest-neighbor interatomic distance, and $P(n)$ the probability for n ^{13}C and $3-n$ ^{12}C atoms to occupy the three nearest-neighbor sites. $\langle M_{2\mathrm{dip}} \rangle = 1.07 \times 10^7$ (rad/s)^2 was used for 30% ^{13}C enrichment of the employed C_{60} sample.

To analyze the evolution of T_1 with T and $\omega/2\pi$, the resulting relaxation rate $T_1^{-1} = T_{1\mathrm{CSA}}^{-1} + T_{1\mathrm{dip}}^{-1}$ was used to fit the experimental data. Here, the correlation time τ is modeled by a thermally activated process following an Arrhenius law, $\tau = \tau_0 \exp(T_0/T)$, where T_0 is the activation energy associated with the C_{60} rotation and τ_0 the preexponential factor. The activation energy for C_{60} rotation inside SWCNTs is determined by not only the C_{60} intermolecular interaction but also the interaction between a C_{60} and the inner wall of the SWCNT. Consequently, the activation energy for the C_{60} molecule is dependent on the SWCNT diameter. Since the present NMR experiments were carried out on the C_{60} peapods with a dispersion of SWCNT diameters, T_1 data were analyzed by assuming a Gaussian spread in T_0, which corresponds to a log-normal distribution of τ.[32] In this case, the relaxation time is expressed as

$$T_1^{-1} = \int \left[T_{1\mathrm{CSA}}^{-1}(T_0') + T_{1\mathrm{dip}}^{-1}(T_0') \right] \frac{1}{\sqrt{2\pi}\beta} \times \exp\left[-\frac{(T_0' - \langle T_0 \rangle)^2}{\beta^2} \right] dT_0'. \tag{4}$$

As demonstrated in Fig. 3, the T and $\omega/2\pi$ dependence of T_1 is successfully explained by taking the parameters of $\tau_0 = 1.62 \times 10^{-12}$ s, $\langle T_0 \rangle = 467$ K, and $\beta = 113$ K. The calculated minimum T_1 value, $T_{1\ \mathrm{min}}$, at $\sim$70 K shows very weak $\omega/2\pi$ dependence: $T_{1\ \mathrm{min}}$ calculated for 42.954 and 100.65 MHz are 1.5 s (at $\sim$65 K) and 0.95 s (at $\sim$70 K), respectively. This is consistent with the experimentally obtained T and $\omega/2\pi$ dependences of T_1 around 70 K.

D. Comparison with other fullerene solids

The measured T dependence of T_1 exhibits no clear deviation from the calculated curves using the same parameters of τ_0, $\langle T_0 \rangle$, and β down to $\sim$30 K, as discussed above. Furthermore, no evidence for anisotropic molecular rotation was found in the NMR spectra in the measured T range. This suggests that the encapsulated C_{60} molecules exhibit a quasi-isotropic rotational motion down to $\sim$30 K without any orientational phase transition, contrary to other fullerene solids.

In solid C_{60}, the C_{60} rotational correlation time significantly increases below $T_C \sim 260$ K,[23–25] resulting in an anomaly in the T dependence of T_1. Similar T_1 anomalies were found in the bulk C_{70} and C_{76} crystals.[29,33] However, in the C_{60} 1D array inside a SWCNT, there is no evidence for the orientational phase transition, as demonstrated in Fig. 4, where the derived τ and its distribution are displayed as a function of the inverse of T, $1/T$. A good measure of the spread of correlation times at each T is given by $\tau = \tau_0 \exp[(\langle T_0 \rangle \pm \beta)/T]$; this range encompasses 84.3% of the distribution. The shaded region in the inset shows this range. In the figure, the T dependences of τ for solid C_{60} (Refs. 23–25) and for ratchet rotation around the molecular long axis in solid C_{70} (Ref. 29) are also shown.

At high T, τ for the C_{60} peapods is nearly the same as that for bulk C_{60} crystals; 5–10 ps in the peapods and 10 ps in

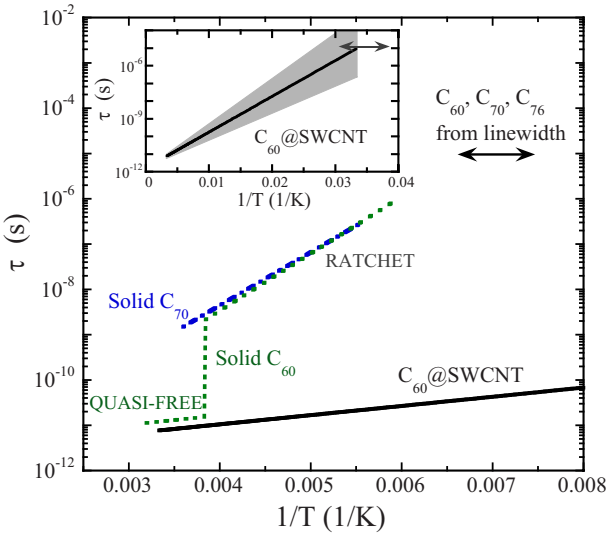

FIG. 4. (Color online) Temperature dependence of rotational correlation time τ for C_{60} encapsulated inside SWCNTs. The solid line denotes $\tau=\tau_0 \exp(\langle T_0\rangle/T)$ with $\tau_0=1.62\times10^{-12}$ s and $\langle T_0\rangle=467$ K. The shaded region in the inset shows the range $\tau=\tau_0 \exp[(\langle T_0\rangle \pm \beta)/T]$ with $\beta=113$ K. In the figure, τ values for quasi-free-rotational phase and ratchet phase in the C_{60} bulk crystals (dotted line) and for the ratchet phase below 280 K in the C_{70} bulk crystals (dash-dotted line) are also displayed for comparison (Refs. 23–25 and 29). The arrows are those estimated from the NMR spectral broadening (Refs. 23, 24, 29, and 33).

the C_{60} crystals. These values are also close to those for the C_{60} gas and C_{60} solution.[34] The evaluated value of $\langle T_0\rangle=467$ K for the C_{60} peapods is also close to 487 K for the quasi-free-rotational phase of solid C_{60} at high T and is much smaller than 2900 K for the ratchet phase below 260 K. This may indicate that the C_{60} molecules inside SWCNTs exhibit a quasi-free-rotational motion at high T. Besides, the C_{60} molecules would be dynamically disordered as in the fcc phase of solid C_{60}.

In the present experiments on the C_{60} peapods, the most surprising observation is the high rotational mobility of C_{60} molecules inside SWCNTs. Bulk solid C_{60}, for example, undergoes an orientational phase transition at $T_C\sim260$ K, and solid C_{70} at ~280 K for the rotation around the C_{70} molecular long axis. These rotational correlation times dramatically increase below their respective T_C and exceed a time scale of NMR linewidth, 10^{-5} s, above 100 K for solid C_{60}, C_{70}, and C_{76}.[23–25,29,33] In the case of the peapods, such T is below 30 K.

The question asked is why the encapsulated C_{60} molecules preserve high rotational mobility down to very low T without any orientational phase transition. One possibility for the absence of a phase transition is that the C_{60} intermolecular interaction is negligibly small compared with the interaction between C_{60} and a SWCNT. However, this is unlikely because the lattice constant, 0.95 nm, for the C_{60} 1D array of peapods is shorter than 1.00 nm of solid C_{60}. Furthermore, the gap between neighboring C_{60} molecules (~2.4 Å) is smaller than that between C_{60} and the nanotube wall (~3.3 Å).[13] Alternatively, it is most plausible that the rotational behavior of C_{60} inside a SWCNT is associated with the 1D nature of the C_{60} array. It is well known that a 1D system with short-range interactions does not undergo a phase transition at finite T. Quite a similar situation has been reported in a C_{70} 1D array inside SWCNTs; an orientational phase transition does not occur due to the 1D nature of the C_{70} array,[13,14] although the encapsulated C_{70} molecule possesses the optimal orientation depending on the SWCNT diameter.[35]

IV. SUMMARY

Molecular rotational dynamics of C_{60} composing a 1D linear array inside SWCNTs has been investigated by ^{13}C NMR in a T range from 4.2 to 300 K. No ^{13}C NMR signal was observed from the sp^3-hybridized carbon expected for 1D polymerization of C_{60} molecules. This result shows that C_{60} molecules exist as monomers inside SWCNTs. The T dependence of T_1 and NMR line shape indicate that the C_{60} molecules may be dynamically disordered and exhibit a large amplitude molecular rotation down to 30 K, much lower than for bulk fullerene solids.[23–25,29,33] The C_{60} linear array inside a SWCNT does not undergo an orientational phase transition, which is associated with its 1D nature.

ACKNOWLEDGMENT

This work was supported in part by a Grant-in-Aid for Scientific Research by the Ministry of Education, Culture, Sports, Science and Technology of Japan.

[1] S. Iijima and T. Ichihashi, Nature (London) **363**, 603 (1993).
[2] M. M. Calbi, M. W. Cole, S. M. Gatica, M. J. Bojan, and G. Stan, Rev. Mod. Phys. **73**, 857 (2001).
[3] X. Fan, E. C. Dickey, P. Eklund, K. Williams, L. Grigorian, R. Buczko, S. T. Pantelides, and S. J. Pennycook, Phys. Rev. Lett. **84**, 4621 (2000).
[4] Y. Maniwa, H. Kataura, M. Abe, S. Suzuki, Y. Achiba, H. Kira, and K. Matsuda, J. Phys. Soc. Jpn. **71**, 2863 (2002).
[5] Y. Maniwa, H. Kataura, M. Abe, A. Udaka, S. Suzuki, Y. Achiba, H. Kira, K. Matsuda, H. Kadowaki, and Y. Okabe, Chem. Phys. Lett. **401**, 534 (2005).
[6] A. N. Khlobystov, D. A. Britz, A. Ardavan, and G. A. Briggs, Phys. Rev. Lett. **92**, 245507 (2004).
[7] B. W. Smith, M. Monthioux, and D. E. Luzzi, Nature (London) **396**, 323 (1998).
[8] S. Okada, S. Saito, and A. Oshiyama, Phys. Rev. Lett. **86**, 3835 (2001).
[9] S. Okada, M. Otani, and A. Oshiyama, Phys. Rev. B **67**, 205411 (2003).
[10] S. Okada, Phys. Rev. B **72**, 153409 (2005).

[11] K. H. Michel, B. Verberck, and A. V. Nikolaev, Phys. Rev. Lett. **95**, 185506 (2005).
[12] B. Verberck and K. H. Michel, Phys. Rev. B **74**, 045421 (2006).
[13] Y. Maniwa, H. Kataura, M. Abe, A. Fujiwara, R. Fujiwara, H. Kira, H. Tou, S. Suzuki, Y. Achiba, E. Nishibori, M. Takata, M. Sakata, and H. Suematsu, J. Phys. Soc. Jpn. **72**, 45 (2003).
[14] Y. Maniwa, H. Kataura, K. Matsuda, and Y. Okabe, New J. Phys. **5**, 127 (2003).
[15] P. A. Heiney, J. E. Fischer, A. R. McGhie, W. J. Romanow, A. M. Denenstein, J. P. McCauley, Jr., A. B. Smith, and D. E. Cox, Phys. Rev. Lett. **66**, 2911 (1991).
[16] H. Kataura, Y. Maniwa, T. Kodama, K. Kikuchi, K. Hirahara, K. Suenaga, S. Iijima, S. Suzuki, Y. Achiba, and W. Kratschmer, Synth. Met. **121**, 1195 (2001).
[17] B. W. Smith, M. Monthioux, and D. E. Luzzi, Chem. Phys. Lett. **315**, 31 (1999).
[18] P. M. Rafailov, C. Thomsen, and H. Kataura, Phys. Rev. B **68**, 193411 (2003).
[19] S. Kawasaki, T. Hara, T. Yokomae, F. Okino, H. Touhara, H. Kataura, T. Watanuki, and Y. Ohishi, Chem. Phys. Lett. **418**, 260 (2006).
[20] M. Chorro1, J. Cambedouzou, A. Iwasiewicz-Wabnig, L. Nóe, S. Rols, M. Monthioux, B. Sundqvist, and P. Launois, Europhys. Lett. **79**, 56003 (2007).
[21] J. Cambedouzou, S. Rols, R. Almairac, J.-L. Sauvajol, H. Kataura, and H. Schober, Phys. Rev. B **71**, 041403(R) (2005).
[22] M. Mehring, *Principles of High Resolution NMR in Solids* (Springer, New York, 1983).
[23] R. Tycko, G. Dabbagh, R. M. Fleming, R. C. Haddon, A. V. Makhija, and S. M. Zahurak, Phys. Rev. Lett. **67**, 1886 (1991).
[24] R. D. Johnson, C. S. Yannoni, H. C. Dorn, J. R. Salem, and D. S. Bethune, Science **255**, 1235 (1992).
[25] Y. Maniwa, M. Nagasaka, A. Ohi, K. Kume, K. Kikuchi, K. Saito, I. Ikemoto, S. Suzuki, and Y. Achiba, Jpn. J. Appl. Phys., Part 2 **33**, L173 (1994).
[26] Y. Iwasa, T. Arima, R. M. Fleming, T. Siegrist, O. Zhou, R. C. Haddon, L. J. Rothberg, K. B. Lyons, H. L. Carter, Jr., A. F. Hebard, R. Tycko, G. Dabbagh, J. J. Krajewski, G. A. Thomas, and T. Yagi, Science **264**, 1570 (1994).
[27] M. Nunez-Regueiro, L. Marques, J.-L. Hodeau, O. Bethoux, and M. Perroux, Phys. Rev. Lett. **74**, 278 (1995).
[28] Y. Maniwa, M. Sato, K. Kume, M. E. Kozlov, and M. Tokumoto, Carbon **34**, 1287 (1996).
[29] Y. Maniwa, A. Ohi, K. Mizoguchi, K. Kume, K. Kikuchi, K. Saito, I. Ikemoto, S. Suzuki, and Y. Achiba, J. Phys. Soc. Jpn. **62**, 1131 (1993).
[30] S. Okada (private communication).
[31] J. H. Van Vleck, Phys. Rev. **74**, 1168 (1948).
[32] A. S. Nowich and B. S. Berry, IBM J. Res. Dev. **5**, 297 (1961).
[33] Y. Maniwa, K. Kume, K. Kikuchi, K. Saito, I. Ikemoto, S. Suzuki, and Y. Achiba, Phys. Rev. B **53**, 14196 (1996).
[34] R. D. Johnson, D. S. Bethune, and C. S. Yannoni, Acc. Chem. Res. **25**, 169 (1992).
[35] M. Chorro, A. Delhey, L. Noe, M. Monthioux, and P. Launois, Phys. Rev. B **75**, 035416 (2007).